International Journal of Mathematics and
Computer Science, **16**(2021), no. 4, 1803–1829

Adapted numerical modeling for advection-reaction-diffusion problems on a bidimensional spatial domain

Raffaele D'Ambrosio[1], Martina Moccaldi[2], Beatrice Paternoster[2]

[1]DISIM - Department of Information Engineering and Computer Science and Mathematics
University of L'Aquila
67100 L'Aquila (AQ), Italy

[2]Department of Mathematics
University of Salerno
84084 Fisciano (SA), Italy

email: raffaele.dambrosio@univaq.it, {mmoccaldi,beapat}@unisa.it

(Received October 27, 2020, Revised April 25, 2021,
Accepted May 28, 2021)

Abstract

The paper provides an adapted numerical scheme for advection-reaction-diffusion problems defined on a bi-dimensional spatial domain. The adaptation is carried out by merging in the numerical scheme the a-priori known informations about the problem, especially those concerning the qualitative behavior of the exact solution and the structure of the system itself. The problem is spatially discretizated through a non-polynomially fitted method of lines, while the time discretization of the resulting system of ODEs (whose vector field consists in both stiff and non-stiff terms) is performed via an implicit-explicit (IMEX) method. The coefficients of the obtained scheme depend on unknown parameters, which need to be properly estimated. In this paper, we propose an estimation strategy based on manipulating the leading term of the local truncation error, whose analytical expression

Key words and phrases: Advection-reaction-diffusion problems, periodic plane wave solutions, trigonometrical fitting, parameter estimation, adapted method of lines, IMEX methods.
AMS (MOS) Subject Classifications: 65M06, 65M12.
ISSN 1814-0432, 2021, http://ijmcs.future-in-tech.net

is also presented. The theoretical analysis is also supported by some numerical tests, confirming the effectiveness of the approach.

1 Introduction

We focus on the numerical integration of advection-reaction-diffusion problems [22, 26], typically modeling chemical interactions among the species of a given system and their transport in space in a flowing medium such as water or air. These systems are widely employed in the applications to describe, for example, air pollution [25, 33], water pollution [2], tumour invasion and metastasis [3], pattern formation [32]. For instance, in air pollution modelling, advection-reaction-diffusion systems involve a large number of species and require numerical schemes able to preserve the qualitative behaviour of the solution. For this reason, an adapted integration is highly recommended.

In general, advection-reaction-diffusion systems exhibit the following expression:

$$\begin{aligned} \partial_t u &= d\,\Delta u + a\,\partial_x u + a\,\partial_y u + f(u), \\ B\,u|_{\partial\Omega} &= b, \\ u(x,y,0) &= \phi(x,y), \end{aligned} \tag{1.1}$$

where $u : \Omega \times [0,T] \longrightarrow \mathbb{R}$ is a state variable denoting, for example, the concentration of a certain biological or chemical species; $\Omega \subset \mathbb{R}^2$ is a bounded domain with sufficiently smooth boundary $\partial\Omega$; f is a smooth function modeling the changes in u due to chemical reactions, emissions (sources) and depositions (sinks); Δu arises from the transport in space of the species; $b : \partial\Omega \times [0,T] \longrightarrow \mathbb{R}$ corresponds to sufficiently smooth boundary data and can be time-dependent; $B = \beta(x)\partial_n + \alpha(x)$ is a first-order differential operator with sufficiently smooth coefficients; the advection coefficient $a : \Omega \times [0,T] \longrightarrow \mathbb{R}$ represents the velocities of the transport medium, such as water or air and the diffusion coefficient $d : \Omega \times [0,T] \longrightarrow \mathbb{R}$ may also include the parametrizations of turbulence. Due to the occurrence of different processes, such systems can exhibit a large range of solutions. In this paper, we particularly focus on problems generating periodic wavefronts.

In the numerical treatment of advection-reaction-diffusion problems, standard numerical schemes could require severe stepsize restrictions in order to accurately reproduce the prescribed oscillatory behaviour of the exact solution along the numerical dynamics. This is due to the fact that they are based on general purpose formulae developed in order to be exact (within round-off error) on algebraic polynomials up to a certain degree. We are

interested in problems having periodic waves as fundamental solutions, so it may be worthwhile to adopt non-polynomially fitted formulae. This idea has given rise to the well-established *exponential fitting* technique (see [20, 23, 27] and references therein). The basis functions are in general assumed to belong to a finite-dimensional space, called fitting space, which is selected according to the a-priori knowledge concerning the exact solution. The resulting adapted method exhibits non-constant coefficients, differently from the traditional case, which depend on parameters characterising the exact solution, whose values are evidently unknown. In this paper, we deal with the two main issues related to the exponential fitting strategy: selecting an appropriate fitting space and properly estimating the unknown parameters. In particular, the prescribed oscillatory dynamics of the considered problems suggests to use a trigonometrical basis. On the other hand, we propose to appropriately manipulate the leading term of the local truncation error in order to approximate the parameters along each spatial direction.

Following [14], we spatially discretize (1.1) through an adapted method of lines based on trigonometrically fitted finite differences and employ an Implicit-Explicit (IMEX) time solver to integrate the resulting system of ordinary differential equations

$$w' = Gw + F(w),$$

where the size of the matrix G relies on the number of spatial grid points and $F(w)$ is a vector-valued function. We observe that in a multidimensional spatial domain, this system may be much larger than in the 1D case, so an efficient time integration is necessary. IMEX schemes are appropriate to integrate such a system, whose vector field contains stiff terms (arising from the diffusion) and non-stiff ones (the non-linear terms arising from the reaction and the advection). An IMEX numerical method implicitly integrates the stiff terms and explicitly ihandlesthe others [1, 28, 34], achieving advantages both in efficiency and stability.

The paper is organized as follows: in Section 2 we develop an adapted numerical method for the general advection-reaction-diffusion system (1.1); Section 3 is devoted to the rigorous analysis of accuracy and stability properties of the presented scheme, while Section 4 concerns the estimate of the parameters appearing in the coefficients of the method and Section 5 exhibits some numerical tests. Finally, Section 6 presents some conclusions and future research perspectives on the topic.

2 An adapted numerical scheme

As announced, we aim to combine an adapted method of lines based on trigonometrically fitted finite differences with an Implicit-Explicit (IMEX) time solver.

Here we assume that diffusion and advection coefficients are constant, the problem (1.1) is provided by Dirichlet boundary conditions and the domain is $\Omega = [0, L]^2$. We discretize (1.1) in space by applying the method of lines (see [24, 29, 30, 31] and references therein), i.e. we select $(N+2)^2$ points in Ω, obtaining the following uniform spatial grid

$$\Omega_h = \{(x_i, y_j) : x_i = ih,\ y_j = jh\ i, j = 0, \dots, N+1,\ h = L/(N+1)\}.$$

The initial value problem related to the resulting semi-discrete system of ordinary differential equations is then the following

$$u'_{ij}(t) = d\,\Delta_n^{(II)}[u_{ij}(t), h] + a\,\Delta_n^{(I)}[u_{ij}(t), h] + f(u_{ij}(t)), \quad i, j = 1, \dots, N, \tag{2.1a}$$

$$u'_{ij}(t) = b'_{ij}(t), \qquad (x_i, y_j) \in \partial\Omega_h, \tag{2.1b}$$

$$u_{ij}(0) = \phi(x_i, y_j), \quad i, j = 0, \dots, N+1, \tag{2.1c}$$

where

$$u_{ij}(t) = u(x_i, y_j, t), \quad i, j = 0, \dots, N+1,$$

and $\Delta_n^{(II)}[u_{ij}(t), h]$ and $\Delta_n^{(I)}[u_{ij}(t), h]$ are the adapted n-point finite differences used to approximate the Laplacian and the sum of first spatial derivatives in (x_i, y_j, t), respectively.

For the construction of such formulae, we follow the well-established exponential fitting procedure [23, 27], which consists in developing formulae in order to be exact (within round-off error) on linearly independent functions other than polynomials. Such basis functions are supposed to belong to a finite-dimensional space called *fitting space* and are selected according to the a-priori knowledge about the qualitative behaviour of the exact solution. We are interested in problems having periodic solutions, so we adopt the following trigonometric space

$$\mathcal{F} = \{1, \sin(\mu_x x), \cos(\mu_x x), \sin(\mu_y y), \cos(\mu_y y)\}, \tag{2.2}$$

where μ_x and μ_y are the spatial frequencies. We adapt the three-point finite difference formula to compute the required spatial derivatives by imposing their exactness on $\mathcal{F}$. We define the linear difference operators

$$\mathcal{L}[h, \mathbf{a}]u = \Delta u - \Delta_3^{(II)}[u, h], \quad \mathcal{L}[h, \mathbf{b}]u = \partial_x u + \partial_y u - \Delta_3^{(I)}[u, h], \tag{2.3}$$

where **a** and **b** are the coefficients of the finite difference formulae $\Delta_3^{(II)}[u,h]$ and $\Delta_3^{(I)}[u,h]$, respectively, and annihilate them on (2.2). This operation gives rise to a linear system in **a** and **b**. Moreover, since the difference operators (2.3) are invariant for translations, it is sufficient to nullify them in $(0,0)$.

The three-point finite difference formula to approximate the Laplacian Δu is defined as follows

$$\Delta_3^{(II)}[u_{ij},h] = \frac{a_0\, u_{i-1\,j} + a_1\, u_{ij} + a_2\, u_{i+1\,j} + a_3\, u_{i\,j-1} + a_4\, u_{i\,j} + a_5\, u_{i\,j+1}}{h^2}, \tag{2.4}$$

where the dependence on time $u_{ij} = u_{ij}(t)$ is omitted for ease of presentation. Similarly to the one-dimensional case [14, 15, 16], imposing its exactness (within round-off error) on functions belonging to the trigonometric fitting space (2.2), we get the following expressions for the coefficients:

$$a_0 = a_2 = \delta_2(z_x), \quad a_3 = a_5 = \delta_2(z_y), \quad a_1 = -2\delta_2(z_x), \quad a_4 = -2\delta_2(z_y), \tag{2.5}$$

where

$$\delta_2(z) = \frac{z^2}{2(1-\cos z)}, \quad z = \mu\, h, \tag{2.6}$$

with $\mu = \mu_x$ or $\mu = \mu_y$ according to the spatial direction. It is noteworthy to highlight that these coefficients are no longer constant, as in traditional finite difference formulae, but depend on the parameters μ_x and μ_y, as it always happens in functionally fitted methods [23]. For z tending to 0, the variable coefficients (2.5) tend to the classic ones

$$a_0 = 1, \quad a_1 = -2, \quad a_2 = 1, \quad a_3 = 1, \quad a_4 = -2, \quad a_5 = 1, \tag{2.7}$$

as expected. As a result, the trigonometrically fitted formula preserves the second order of accuracy of its classic counterpart.

In a similar way, the three-point finite difference formula

$$\Delta_3^{(I)}[u_{ij},h] = \frac{b_0\, u_{i-1\,j} + b_1\, u_{ij} + b_2\, u_{i+1\,j} + b_3\, u_{i\,j-1} + b_4\, u_{i\,j} + b_5\, u_{i\,j+1}}{h}, \tag{2.8}$$

for the approximation of the sum of the first spatial derivatives is depends on the following coefficients

$$b_0 = -\frac{\delta_1(z_x)}{2}, \quad b_1 = 0 = b_4, \quad b_2 = \frac{\delta_1(z_x)}{2}, \quad b_3 = -\frac{\delta_1(z_y)}{2}, \quad b_5 = \frac{\delta_1(z_y)}{2}, \tag{2.9}$$

where

$$\delta_1(z) = \frac{z}{\sin z}, \quad z = \mu\, h, \tag{2.10}$$

with $\mu = \mu_x$ or $\mu = \mu_y$ according to the spatial direction. Also in this case,for z tending to 0, the coefficients tend to the classic values

$$b_0 = -\frac{1}{2}, \quad b_1 = 0, \quad b_2 = \frac{1}{2}, \quad b_3 = -\frac{1}{2}, \quad b_4 = 0, \quad b_5 = \frac{1}{2}. \tag{2.11}$$

Therefore, the trigonometrically fitted formula conserves the second order of accuracy of the corresponding classic one.

For the time integration, it is convenient to recast system (2.1a)-(2.1b) in a more compact form. For this purpose, we consider the following matrices

$$A = \begin{bmatrix} -2 & 1 & & & \\ 1 & -2 & 1 & & \\ & \ddots & \ddots & \ddots & \\ & & 1 & -2 & 1 \\ & & & 1 & -2 \end{bmatrix}, \qquad B = \begin{bmatrix} 0 & 1 & & & \\ -1 & 0 & 1 & & \\ & \ddots & \ddots & \ddots & \\ & & -1 & 0 & 1 \\ & & & -1 & 0 \end{bmatrix}, \tag{2.12}$$

and we construct the matrices $\mathcal{A}$ and $\mathcal{B}$ according to the kind of three-point finite difference formulae employed to approximate the differential operators involved, as follows:

- *classic three-point finite difference formulae:*

$$\mathcal{A} = \frac{1}{h^2}\left(\mathbb{I} \otimes A + A \otimes \mathbb{I}\right), \quad \mathcal{B} = \frac{1}{2h}\left(\mathbb{I} \otimes B + B \otimes \mathbb{I}\right); \tag{2.13}$$

- *trigonometrically fitted three-point finite difference formulae with the same spatial frequency in both spatial directions, i.e.* $\mu_x = \mu = \mu_y$ *and* $z_x = z_y = \mu\, h$*:*

$$\begin{aligned} \mathcal{A}(z) &= \frac{\delta_2(z)}{h^2}\left(\mathbb{I} \otimes A + A \otimes \mathbb{I}\right), \quad \delta_2(z) = \frac{z^2}{2(1-\cos z)}, \\ \mathcal{B}(z) &= \frac{\delta_1(z)}{2h}\left(\mathbb{I} \otimes B + B \otimes \mathbb{I}\right), \quad \delta_1(z) = \frac{z}{\sin z}; \end{aligned} \tag{2.14}$$

- *trigonometrically fitted three-point finite difference formulae with different spatial frequencies* μ_x *and* μ_y*:*

$$\begin{aligned} \mathcal{A}(z_x, z_y) &= \frac{1}{h^2}\left(\mathbb{I} \otimes \delta_2(z_x)\, A + A \otimes \delta_2(z_y)\, \mathbb{I}\right), \quad \delta_2(z) = \frac{z^2}{2(1-\cos z)}, \\ \mathcal{B}(z_x, z_y) &= \frac{1}{2h}\left(\mathbb{I} \otimes \delta_1(z_x)\, B + B \otimes \delta_1(z_y)\, \mathbb{I}\right), \quad \delta_1(z) = \frac{z}{\sin z}, \end{aligned} \tag{2.15}$$

where $z = \mu h$, $z_x = \mu_x h$ and $z_y = \mu_y h$.

Correspondingly, the system (2.1a)-(2.1b) becomes

$$U'(t) = d\,\mathcal{A}(z)\,U(t) + a\,\mathcal{B}(z)\,U(t) + F(U(t)) + \mathcal{S}, \tag{2.16}$$

where U contains the values of the functions $u_{ij}(t)$ defined on each spatial grid point

$$U(t) = [u_{11}(t),\ u_{21}(t),\ \ldots,\ u_{N1}(t),\quad \ldots\quad u_{1N}(t),\ u_{2N}(t),\ \ldots,\ u_{NN}(t)]^{\intercal},$$

$F(U(t))$ contains the values assumed by the reaction term f in the vector U

$$F(U(t))_\xi = f(U(t)_\xi),$$

and the vector $\mathcal{S}$ includes terms deriving from combining differentiation formulae with boundary conditions and thus depends on the boundary data b:

$$S = [\sigma_1\ b(t, \underline{x}, y_0) + S_1,\quad S_2,\quad \ldots,\quad S_{N-1},\quad \sigma_2\ b(t, \underline{x}, y_{N+1}) + S_N]^{\intercal},$$

with $\underline{x} = [x_1, \ldots, x_N]^{\intercal}$, $S_\xi = [\sigma_3\ b(t, x_0, y_\xi),\ 0,\ \ldots,\ 0,\ \sigma_4\ b(t, x_{N+1}, y_\xi)]^{\intercal}$. The quantities σ_ξ are defined in a different way according to the employed finite difference, as follows:

- *classic three-point finite difference formula:*

$$\sigma_1 = \frac{d}{h^2} - \frac{a}{2h} = \sigma_3, \quad \sigma_2 = \frac{d}{h^2} + \frac{a}{2h} = \sigma_4;$$

- *trigonometrically fitted three-point finite difference formula with the same spatial frequency in both spatial directions, i.e.* $\mu_x = \mu = \mu_y$ *and* $z_x = z_y = \mu\, h$*:*

$$\sigma_1 = \frac{d\,\delta_2(z)}{h^2} - \frac{a\,\delta_1(z)}{2h} = \sigma_3, \quad \sigma_2 = \frac{d\,\delta_2(z)}{h^2} + \frac{a\,\delta_1(z)}{2h} = \sigma_4;$$

- *trigonometrically fitted three-point finite difference formula with different spatial frequencies* μ_x *and* μ_y*:*

$$\sigma_1 = \frac{d\,\delta_2(z_y)}{h^2} - \frac{a\,\delta_1(z_y)}{2h}, \quad \sigma_2 = \frac{d\,\delta_2(z_y)}{h^2} + \frac{a\,\delta_1(z_y)}{2h},$$
$$\sigma_3 = \frac{d\,\delta_2(z_x)}{h^2} - \frac{a\,\delta_1(z_x)}{2h}, \quad \sigma_4 = \frac{d\,\delta_2(z_x)}{h^2} + \frac{a\,\delta_1(z_x)}{2h}.$$

2.1 Time integration by IMEX methods

As already highlighted, the whole mechanism behind an advection-reaction-diffusion problem is based on the occurrence of different phenomena. This mixed nature is transferred into the corresponding mathematical model and, in particular, in the vector field of the system of ODEs (2.16). Indeed, its component stemming from the diffusion is typically much more stiff than the constituents deriving from the advection and the reaction [1, 22, 34]. A totally explicit scheme would prescribe a strong stepsize restriction in order to guarantee the stability in case of stiff systems. On the other hand, a totally implicit method would better treat the stiffness, but it would increase the computational effort and complicate the implementation, especially in presence of non-linearities in the reaction term. For these reasons, when the vector field contains several parts of different natures, it may be worthwhile to adopt an implicit-explicit (IMEX) scheme (see, for instance, [1, 4, 5, 6, 28, 34]), which integrates implicitly only the terms that need it (the stiff ones) and explicitly the other ones, thus gaining advantages both in stability and efficiency.

Following this idea, we discretize the time interval $[0, T]$ through a uniform grid of M points

$$t_m = m\,k, \quad m = 0, 1, \ldots, M-1,$$

with constant stepsize k and we integrate system (2.16) by employing the IMEX Euler method, as follows:

$$U^{m+1} = U^m + k\,d\,\mathcal{A}^{m+1}U^{m+1} + k\,a\,\mathcal{B}^m U^m + k\,F(U^m) + k\,\mathcal{S}_d^{m+1} + k\,\mathcal{S}_a^m, \quad (2.17)$$

i.e. we implicitly integrate the term deriving from the diffusion (which is typically stiff) and explicitly integrate the other ones. We remark that the vector $\mathcal{S}$ includes terms deriving from combining differentiation formulae and boundary conditions, so it is composed by a term $\mathcal{S}_d$ related to the diffusion and a constituent $\mathcal{S}_a$ linked to the advection, which are implicitly or explicitly integrated, respectively. Moreover, the matrices $\mathcal{A}$ and $\mathcal{B}$ and the vector $\mathcal{S}$ rely on the parameters μ_x and μ_y, which have to be estimated if they are unknown. The selection strategy is described in Section 4.

3 Accuracy and stability analysis

In this section, we analyse accuracy and stability properties of the method (2.17), denoted as IMEX-EF henceforth. For this purpose, we investigate

the general case of a different frequency in each spatial direction. For ease of presentation, we adopt the following notation:

$$\delta_1(z_x) = \delta_1^x, \quad \delta_1(z_y) = \delta_1^y, \quad \delta_2(z_x) = \delta_2^x, \quad \delta_2(z_y) = \delta_2^y, \tag{3.1}$$

where we remark that $\delta_1(z)$ and $\delta_2(z)$ are defined as follows:

$$\delta_1(z) = \frac{z}{\sin z}, \quad \delta_2(z) = \frac{z^2}{2(1-\cos z)}. \tag{3.2}$$

In particular, Theorem 3.1 shows that the order of consistency of the numerical scheme is $\mathcal{O}(k) + \mathcal{O}(z_x^2) + \mathcal{O}(z_y^2) + \mathcal{O}(z_x^2\, k) + \mathcal{O}(z_y^2\, k)$. This result is coherent with the theoretical expectations since the fitted finite difference formulae used to approximate spatial derivatives have order 2 and depend on z_x and z_y and the IMEX-Euler method has order 1.

Theorem 3.1. *The IMEX-EF method* (2.17) *is consistent with problem* (1.1) *and the order of consistency is* $\mathcal{O}(k) + \mathcal{O}(z_x^2) + \mathcal{O}(z_y^2) + \mathcal{O}(z_x^2\, k) + \mathcal{O}(z_y^2\, k)$, *where* $z_x = \mu_x h$ *and* $z_y = \mu_y h$, μ_x *and* μ_y *are the spatial frequencies,* h *is the spatial mesh width and* k *is the time stepsize.*

Proof. We define the local truncation error at the $(i, j, m+1)$ grid point by

$$\begin{aligned} P_{h,k}^{i,j,m+1}[u] = {} & \frac{u_{ij}^{m+1} - u_{ij}^m}{k} - \frac{d\,\delta_2^x}{h^2}\left(u_{i+1\,j}^{m+1} - 2u_{ij}^{m+1} + u_{i-1\,j}^{m+1}\right) \\ & - \frac{d\,\delta_2^y}{h^2}\left(u_{i\,j+1}^{m+1} - 2u_{ij}^{m+1} + u_{i\,j-1}^{m+1}\right) \\ & - \frac{a\delta_1^x}{2h}\left(u_{i+1\,j}^m - u_{i-1\,j}^m\right) - \frac{a\delta_1^y}{2h}\left(u_{i\,j+1}^m - u_{i\,j-1}^m\right) - f\left(u_{ij}^m\right), \end{aligned} \tag{3.3}$$

where $u_{ij}^m = u(x_i, y_j, t_m)$ and δ_1 and δ_2 are defined in (3.1) and (3.2). We

expand in Taylor series the following terms:

$$u_{ij}^{m+1} = u_{ij}^{m} + k\left(\frac{\partial u}{\partial t}\right)_{i,j}^{m} + \frac{k^2}{2}\left(\frac{\partial^2 u}{\partial t^2}\right)_{i,j}^{m} + \mathcal{O}(k^3), \tag{3.4a}$$

$$u_{i+1,j}^{n} = u_{ij}^{n} + h\left(\frac{\partial u}{\partial x}\right)_{i,j}^{n} + \frac{h^2}{2}\left(\frac{\partial^2 u}{\partial x^2}\right)_{i,j}^{n} + \mathcal{O}(h^3), \quad \forall n \tag{3.4b}$$

$$u_{i-1,j}^{n} = u_{ij}^{n} - h\left(\frac{\partial u}{\partial x}\right)_{i,j}^{n} + \frac{h^2}{2}\left(\frac{\partial^2 u}{\partial x^2}\right)_{i,j}^{n} + \mathcal{O}(h^3), \quad \forall n \tag{3.4c}$$

$$u_{i,j+1}^{n} = u_{ij}^{n} + h\left(\frac{\partial u}{\partial y}\right)_{i,j}^{n} + \frac{h^2}{2}\left(\frac{\partial^2 u}{\partial y^2}\right)_{i,j}^{n} + \mathcal{O}(h^3), \quad \forall n \tag{3.4d}$$

$$u_{i,j-1}^{n} = u_{ij}^{n} - h\left(\frac{\partial u}{\partial y}\right)_{i,j}^{n} + \frac{h^2}{2}\left(\frac{\partial^2 u}{\partial y^2}\right)_{i,j}^{n} + \mathcal{O}(h^3), \quad \forall n \tag{3.4e}$$

$$\left(\frac{\partial^2 u}{\partial x^2}\right)_{i,j}^{m+1} = \left(\frac{\partial^2 u}{\partial x^2}\right)_{i,j}^{m} + k\left[\frac{\partial}{\partial t}\left(\frac{\partial^2 u}{\partial x^2}\right)\right]_{i,j}^{m} + \frac{k^2}{2}\left[\frac{\partial^2}{\partial t^2}\left(\frac{\partial^2 u}{\partial x^2}\right)\right]_{i,j}^{m} + \mathcal{O}(k^3), \tag{3.4f}$$

$$\left(\frac{\partial^2 u}{\partial y^2}\right)_{i,j}^{m+1} = \left(\frac{\partial^2 u}{\partial y^2}\right)_{i,j}^{m} + k\left[\frac{\partial}{\partial t}\left(\frac{\partial^2 u}{\partial y^2}\right)\right]_{i,j}^{m} + \frac{k^2}{2}\left[\frac{\partial^2}{\partial t^2}\left(\frac{\partial^2 u}{\partial y^2}\right)\right]_{i,j}^{m} + \mathcal{O}(k^3). \tag{3.4g}$$

Equation (3.4a) is equivalent to

$$\frac{u_{ij}^{m+1} - u_{ij}^{m}}{k} = \left(\frac{\partial u}{\partial t}\right)_{i,j}^{m} + \frac{k}{2}\left(\frac{\partial^2 u}{\partial t^2}\right)_{i,j}^{m} + \mathcal{O}(k^2).$$

Summing equations (3.4b)-(3.4e) for $n = m + 1$ and taking into account (3.4f)-(3.4g), we obtain

$$\begin{aligned} u_{i+1\,j}^{m+1} - 2u_{i\,j}^{m+1} + u_{i-1\,j}^{m+1} + u_{i\,j+1}^{m+1} - 2u_{i\,j}^{m+1} + u_{i\,j-1}^{m+1} \\ = h^2\left((\Delta u)_{ij}^{m} + k\frac{\partial}{\partial t}(\Delta u)_{ij}^{m} + \mathcal{O}(k^2)\right) + \mathcal{O}(h^4), \end{aligned}$$

whereas subtracting equation (3.4c) from equation (3.4b) and equation (3.4e) from equation (3.4d) for $n = m$, we achieve

$$u_{i+1\,j}^{m} - u_{i-1\,j}^{m} + u_{i\,j+1}^{m} - u_{i\,j-1}^{m} = 2h\left(\frac{\partial u}{\partial x} + \frac{\partial u}{\partial y}\right)_{i,j}^{m} + \mathcal{O}(h^4)\,.$$

We now expand $\delta_1(z)$ and $\delta_2(z)$ in power series as follows

$$\delta_1(z) = 1 + \frac{z^2}{6} + \frac{7z^4}{360} + \mathcal{O}(z^6), \qquad \delta_2(z) = 1 + \frac{z^2}{12} + \frac{z^4}{240} + \mathcal{O}(z^6)\,.$$

Therefore, the local truncation error (3.3) assumes the following expression:

$$\begin{aligned}
P_{h,k}^{i,j,m+1}[u] = & \left(\frac{\partial u}{\partial t}\right)_{i,j}^{m} + \frac{k}{2}\left(\frac{\partial^2 u}{\partial t^2}\right)_{i,j}^{m} + \mathcal{O}(k^2) - f(u_{ij}^m) \\
& - d\left[1 + \frac{z_x^2}{12} + \mathcal{O}(z_x^4)\right]\left[\left(\frac{\partial^2 u}{\partial x^2}\right)_{i,j}^{m} + k\left(\frac{\partial}{\partial t}\left(\frac{\partial^2 u}{\partial x^2}\right)\right)_{i,j}^{m} + \mathcal{O}(k^2) + \mathcal{O}(h^2)\right] \\
& - d\left[1 + \frac{z_y^2}{12} + \mathcal{O}(z_y^4)\right]\left[\left(\frac{\partial^2 u}{\partial y^2}\right)_{i,j}^{m} + k\left(\frac{\partial}{\partial t}\left(\frac{\partial^2 u}{\partial y^2}\right)\right)_{i,j}^{m} + \mathcal{O}(k^2) + \mathcal{O}(h^2)\right] \\
& - a\left[1 + \frac{z_x^2}{6} + \mathcal{O}(z_x^4)\right]\left[\left(\frac{\partial u}{\partial x}\right)_{i,j}^{m} + \mathcal{O}(h^3)\right] \\
& - a\left[1 + \frac{z_y^2}{6} + \mathcal{O}(z_y^4)\right]\left[\left(\frac{\partial u}{\partial y}\right)_{i,j}^{m} + \mathcal{O}(h^3)\right] \\
& = \left(\frac{\partial u}{\partial t}\right)_{i,j}^{m} - d\,(\Delta u)_{i,j}^{m} - a\left(\frac{\partial u}{\partial x} + \frac{\partial u}{\partial y}\right)_{i,j}^{m} - f\left(u_{ij}^m\right) \\
& + k\left[\frac{1}{2}\frac{\partial^2 u}{\partial t^2} - d\frac{\partial}{\partial t}(\Delta u)\right]_{i,j}^{m} + \mathcal{O}(k^2) + \mathcal{O}(h^2) \\
& - z_x^2\left[\frac{d}{12}\,\frac{\partial^2 u}{\partial x^2} + \frac{a}{6}\,\frac{\partial u}{\partial x}\right]_{i,j}^{m} - z_y^2\left[\frac{d}{12}\,\frac{\partial^2 u}{\partial y^2} + \frac{a}{6}\,\frac{\partial u}{\partial y}\right]_{i,j}^{m} + \mathcal{O}(z_x^4) + \mathcal{O}(z_y^4) \\
& - z_x^2\,k\left[\frac{d}{12}\,\frac{\partial}{\partial t}\frac{\partial^2 u}{\partial x^2}\right]_{i,j}^{m} - z_y^2\,k\left[\frac{d}{12}\,\frac{\partial}{\partial t}\frac{\partial^2 u}{\partial y^2}\right]_{i,j}^{m} + \mathcal{O}(z_x^2\,k^2) + \mathcal{O}(z_y^2\,k^2).
\end{aligned}$$

Since u is the exact solution of problem (1.1), the following equation is verified

$$\left(\frac{\partial u}{\partial t}\right)_{i,j}^{m} - d\,(\Delta u)_{i,j}^{m} - a\left(\frac{\partial u}{\partial x} + \frac{\partial u}{\partial y}\right)_{i,j}^{m} - f\left(u_{ij}^m\right) = 0,$$

so the local truncation error is

$$P_{h,k}^{i,j,m+1}[u] = \mathcal{O}(k) + \mathcal{O}(z_x^2) + \mathcal{O}(z_y^2) + \mathcal{O}(z_x^2\,k) + \mathcal{O}(z_y^2\,k). \qquad (3.5)$$

□

Theorem 3.1 also allows us to prove that the numerical scheme (2.17) is convergent, as shown in the following theorem.

Theorem 3.2. *If the vector valued function $F(U(t))$ is smooth enough and its gradient is bounded*

$$\|\nabla F\|_2 \leq F_{max}\,,$$

then, IMEX-EF method (2.17) *is convergent.*

Proof. The discretization error in a fixed time grid point t_{m+1} is

$$E^{m+1} = U(t_{m+1}) - U^{m+1}, \tag{3.6}$$

where $U(t_{m+1})$ is the exact solution in t_{m+1} and U^{m+1} is the numerical solution in the same grid point computed by method (2.17). Consistency of the method (see Theorem 3.1) leads to

$$\begin{aligned} U(t_{m+1}) = U(t_m) + k\,d\,\mathcal{A}\,U(t_{m+1}) + k\;a\,\mathcal{B}U(t_m) \\ + k\,F(U(t_m)) + k\,S_d^{m+1} + k\,S_a^m + \mathcal{R}_{z,k}^{m+1}, \end{aligned} \tag{3.7}$$

where $\mathcal{R}_{z,k}^{m+1} = \mathcal{O}(k) + \mathcal{O}(z_x^2) + \mathcal{O}(z_y^2) + \mathcal{O}(z_x^2\;k) + \mathcal{O}(z_y^2\;k)$, $z_x = \mu_x h$, $z_y = \mu_y h$, h is the spatial mesh grid and k is the time stepsize. We assume that the frequencies μ_x and μ_y are known, so the matrices $\mathcal{A}$ and $\mathcal{B}$ are fixed. Moreover, the vectors S_d and S_a depend only on time in case of time-dependent boundary data b.
Hence, the discretization error (3.6) assumes the following expression

$$\begin{aligned} E^{m+1} &= U(t_m) + k\,d\,\mathcal{A}\,U(t_{m+1}) + k\,\mathcal{B}U(t_m) + k\;F(U(t_m)) + \mathcal{R}_{z,k}^{m+1} \\ &\quad - U^m - k\,d\,\mathcal{A}\,U^{m+1} - k\,a\,\mathcal{B}U^m - k\,F(U^m) \\ &= E^m + k\,d\,\mathcal{A}\,E^{m+1} + k\,a\,\mathcal{B}E^m + k\,(F(U(t_m)) - F(U^m)) + \mathcal{R}_{z,k}^{m+1}. \end{aligned}$$

In order to bound its norm, we first observe that by assumption F is smooth enough, so we can apply the Mean Value Theorem:

$$\|F(U(t_m)) - F(U^m)\|_2 = \|\nabla F\|_2\,\|U(t_m) - U^m\|_2 = \|\nabla F\|_2\,\|E^m\|_2\,.$$

The hypothesis $\|\nabla F\|_2 \leq F_{max}$ implies also that

$$\|F(U(t_m)) - F(U^m)\|_2 \leq F_{max}\,\|E^m\|_2\,. \tag{3.8}$$

Due to its symmetry, the matrix $\mathcal{A}$ can be factorized through an orthogonal matrix V and a diagonal matrix Λ having the eigenvalues of $\mathcal{A}$ as elements, as follows:

$$\mathcal{A} = V\Lambda V^{\intercal},$$

which leads to a similar decomposition for the matrix $\mathbb{I} - kd\mathcal{A}$:

$$\mathbb{I} - kd\mathcal{A} = V(\mathbb{I} - kd\Lambda)V^{\intercal}.$$

Since the elements of the diagonal matrix $\mathbb{I} - kd\Lambda$ verify

$$l_s = 1 + \frac{4kd}{h^2}\left(\delta_2^x + \delta_2^y\right)\sin^2\frac{s\pi}{2(N+1)} > 0, \quad s = 1, \ldots, N, \tag{3.9}$$

the matrix $\mathbb{I} - ka\Lambda$, and, as a consequence, the matrix $\mathbb{I} - kd\mathcal{A}$ are invertible, so the discretization error can be explicitly expressed as follows:

$$E^{m+1} = (\mathbb{I} - k\,d\,\mathcal{A})^{-1}\left[(\mathbb{I} + k\,a\,\mathcal{B})E^m + k\left(F(U(t_m)) - F(U^m)\right) + \mathcal{R}_{z,k}^{m+1}\right]. \tag{3.10}$$

We next observe that

$$\left\|(\mathbb{I} - k\,d\,\mathcal{A})^{-1}\right\|_2 \leq \ \|V\|_2\ \left\|(\mathbb{I} - k\,d\,\Lambda)^{-1}\right\|_2\ \|V^{\intercal}\|_2 \leq 1, \tag{3.11}$$

being V orthonormal and the eigenvalues of the diagonal matrix $(\mathbb{I} - k\,d\,\Lambda)^{-1}$ less or equal than 1. Finally, since $\|\mathcal{B}\|_2 = \rho(\mathcal{B})$ for the antisymmetry, the following condition holds

$$\|\mathcal{B}\|_2 \leq \frac{\delta_1^x + \delta_1^y}{h}. \tag{3.12}$$

Hence, taking into account conditions (3.8), (3.11) and (3.12), we can obtain an upper bound for the norm of the discretization error:

$$\left\|E^{m+1}\right\|_2 \leq \left(1 + \frac{k}{h}a\left(\delta_1^x + \delta_1^y\right) + kF_{max}\right)\ \|E^m\|_2\ + \left\|\mathcal{R}_{z,k}^{m+1}\right\|_2. \tag{3.13}$$

We employ the following notation

$$Q = 1 + \frac{k}{h}a\left(\delta_1^x + \delta_1^y\right) + kF_{max}, \tag{3.14}$$

and recursively apply Equation (3.13) until obtaining the discretization error at first step, as follows:

$$\left\|E^{m+1}\right\|_2 \leq Q^{m+1}\left\|E^0\right\|_2 + \sum_{s=1}^{m+1}\left\|\mathcal{R}_{z,k}^{s}\right\|_2 Q^{m+1-s}.$$

Since $\|E^0\|_2 = 0$, the following inequality holds for each m and under the hypothesis that k and h are comparable:

$$\left\|E^{m+1}\right\|_2 \leq \sum_{s=1}^{m+1} \left\|\mathcal{R}_{z,k}^s\right\|_2 Q^{m+1-s} \xrightarrow[h,k\to 0]{} 0.$$

□

Finally, we investigate the stability of the numerical scheme (2.17).

Theorem 3.3. *Assume that the vector valued function $F(U(t_m))$ is smooth enough and satisfies the bound*

$$\|\nabla F\|_2 \leq F_{max}. \tag{3.15}$$

If

$$\left\|(\mathbb{I} - kd\mathcal{A})^{-1}\right\|_2 (\|\mathbb{I} + ka\mathcal{B}\|_2 + kF_{max}) \leq 1, \tag{3.16}$$

then the method (2.17) *is stable, where h is the spatial mesh width, k is the time stepsize, a and d are the advection and diffusion coefficients, respectively.*

Proof. In [31] a method is said to be stable if the error caused by an incoming perturbation does not blow up. For this reason, we perturb the solution U^m at time $t = t_m$ as follows

$$\widetilde{U}^m = U^m + \delta,$$

and we consider the error $E^{m+1} = U^{m+1} - \widetilde{U}^{m+1}$ due to this perturbation:

$$E^{m+1} = (\mathbb{I} - kd\mathcal{A})^{-1} \left(\mathbb{I} + ka\mathcal{B} + k\left(F(U^m) - F(\widetilde{U}^m)\right)\right) E^m.$$

Since by assumption the reaction term F is smooth enough and exhibits a bounded gradient (3.15), the following inequality holds

$$\left\|F(U^m) - F(\widetilde{U}^m)\right\|_2 \leq \|\nabla F\|_2 \left\|E^m\right\|_2 \leq F_{max} \left\|E^m\right\|_2, \tag{3.17}$$

which leads to the following upper bound for the norm of the perturbation error

$$\left\|E^{m+1}\right\|_2 \leq \left\|(\mathbb{I} - kd\mathcal{A})^{-1}\right\|_2 (\|\mathbb{I} + ka\mathcal{B}\|_2 + kF_{max}) \left\|E^m\right\|_2.$$

This stability inequality implies the stability condition

$$\left\|(\mathbb{I} - kd\mathcal{A})^{-1}\right\|_2 (\|\mathbb{I} + ka\mathcal{B}\|_2 + kF_{max}) \leq 1,$$

that gives the thesis. □

4 Parameter selection

We have already observed that the coefficients (2.5) and (2.9) of the adapted formulae for the approximation of the spatial derivatives depend on the parameters μ_x and μ_y characterizing the exact solution and generally unknown. In this section, we describe a procedure to estimate these parameters based on annihilating the leading term of the local truncation error, whose expression at each grid point is the following, as shown in the proof of Theorem 3.1:

$$\begin{aligned} P_{h,k}^{i,j,m+1}[u] = k \left[\frac{1}{2}\frac{\partial^2 u}{\partial t^2} - d\frac{\partial}{\partial t}(\Delta u)\right]_{i,j}^{m} + \mathcal{O}(k^2) + \mathcal{O}(h^2) \\ - z_x^2 \left[\frac{d}{12}\,\frac{\partial^2 u}{\partial x^2} + \frac{a}{6}\,\frac{\partial u}{\partial x}\right]_{i,j}^{m} - z_y^2 \left[\frac{d}{12}\,\frac{\partial^2 u}{\partial y^2} + \frac{a}{6}\,\frac{\partial u}{\partial y}\right]_{i,j}^{m} + \mathcal{O}(z_x^4) + \mathcal{O}(z_y^4) \\ - z_x^2\, k \left[\frac{d}{12}\,\frac{\partial}{\partial t}\frac{\partial^2 u}{\partial x^2}\right]_{i,j}^{m} - z_y^2\, k \left[\frac{d}{12}\,\frac{\partial}{\partial t}\frac{\partial^2 u}{\partial y^2}\right]_{i,j}^{m} + \mathcal{O}(z_x^2\, k^2) + \mathcal{O}(z_y^2\, k^2). \end{aligned}$$

We first consider the z_x-dependent leading term

$$\mathcal{T}^{i,j,m+1}(z_x) = -z_x^2 \left[\frac{d}{12}\left(\frac{\partial^2 u}{\partial x^2}\right) + \frac{a}{6}\left(\frac{\partial u}{\partial x}\right) + k\frac{d}{12}\left(\frac{\partial}{\partial t}\frac{\partial^2 u}{\partial x^2}\right)\right]_{ij}^{m}, \qquad (4.1)$$

and we approximate the involved spatial derivatives through the trigonometrically fitted finite difference formulae (2.4) and (2.8) with coefficients (2.5) and (2.9), obtaining

$$\mathcal{T}^{i,j,m+1}(z_x) \approx \overline{T}^{i,j,m+1}(z_x) = -\frac{\mu_x^2}{12}\left(d\,\delta_2^x\,(2\alpha_{ij}^m - \alpha_{ij}^{m-1}) + a\,h\,\delta_1^x\,\beta_{i,j}^m\right), \qquad (4.2)$$

where

$$\alpha_{ij}^m = u_{i+1j}^m - 2u_{ij}^m + u_{i-1j}^m, \quad \beta_{ij}^m = u_{i+1j}^m - u_{i-1j}^m. \qquad (4.3)$$

An estimate for the parameter μ_x is provided by annihilating $\overline{T}^{i,j,m+1}(z_x)$, which approximates the z_x-dependent leading term of the local truncation error. This is equivalent to solving the following nonlinear equation

$$d\,\frac{z_x^2}{2(1-\cos z_x)}\,(2\alpha_{ij}^m - \alpha_{ij}^{m-1}) + a\,h\,\frac{z_x}{\sin z_x}\,\beta_{i,j}^m = 0,$$

which, considering the McLaurin expansion of the functions $\sin z_x$ and $1-\cos z_x$ truncated at the fourth order term, becomes

$$d\left(1-\frac{z_x^2}{6}\right)\,(2\alpha_{ij}^m-\alpha_{ij}^{m-1})+a\,h\,\beta_{i,j}^m\left(1-\frac{z_x^2}{12}\right)=0,$$

whose solutions are

$$z_x=\pm\sqrt{6+\frac{6ah\,\beta_{i,j}^m}{2d\,(2\alpha_{ij}^m-\alpha_{ij}^{m-1})+ah\,\beta_{i,j}^m}}.$$

Hence, an estimate for the parameter μ is the following

$$\tilde{\mu}_x=\frac{1}{h}\sqrt{6+\frac{6ah\,|\beta_{i,j}^m|}{2d\,|2\alpha_{ij}^m-\alpha_{ij}^{m-1}|+ah\,|\beta_{i,j}^m|}}. \tag{4.4}$$

To improve this estimate, we add a control factor $\zeta>0$ such that

$$\frac{C_{i,j}^m\,\zeta^2}{h^2}\le 1,\qquad C_{i,j}^m=9\left(1+\frac{ah\,|\beta_{i,j}^m|}{2d\,|2\alpha_{ij}^m-\alpha_{ij}^{m-1}|+ah\,|\beta_{i,j}^m|}\right). \tag{4.5}$$

Indeed, the following relation is verified:

$$\left|\mathcal{T}^{i,j,\,m+1}\,(\zeta\tilde{\mu}_x h)\right|=\zeta^2\,C_{i,j}^m\,D_{i,j}^m\le\frac{\zeta^2\,C_{i,j}^m}{h^2}\,D_{i,j}^m\le D_{i,j}^m\le C_{i,j}^m\,D_{i,j}^m=\left|\mathcal{T}^{i,j,\,m+1}(\tilde{\mu}_x h)\right|, \tag{4.6}$$

being $C_{i,j}\ge 1$ for the definition (4.5), $\mathcal{T}^{i,j,\,m+1}$ the leading term of the local truncation error given by (4.1) and

$$D_{i,j}^m=\frac{1}{18}\left|d\left(\frac{\partial^2 u}{\partial x^2}+k\frac{\partial}{\partial t}\frac{\partial^2 u}{\partial x^2}\right)_{i,j}^m+2a\left(\frac{\partial u}{\partial x}\right)_{i,j}^m\right|. \tag{4.7}$$

From (4.6), the leading term of the local truncation error $\mathcal{T}^{i,j,\,m+1}$ assumes a smaller value in $\zeta\tilde{\mu}_x h$ than in $\tilde{\mu}_x h$, so the control factor ζ allows us to construct an improved estimate for the parameter μ_x:

$$\mu_x=\zeta\tilde{\mu}_x=\frac{\zeta}{h}\sqrt{6+\frac{6ah\,|\beta_{i,j}^m|}{2d\,|2\alpha_{ij}^m-\alpha_{ij}^{m-1}|+ah\,|\beta_{i,j}^m|}},\qquad \zeta=\frac{h}{1.05+2(d+a)} \tag{4.8}$$

where α_{ij}^m and β_{ij}^m are defined in (4.3) and ζ is computed by employing condition (4.5).

Similarly, we consider the z_y-dependent leading term of the local truncation error

$$\mathcal{T}^{i,\,j,\,m+1}(z_y) = -z_y^2 \left[\frac{d}{12} \left(\frac{\partial^2 u}{\partial y^2} \right) + \frac{a}{6} \left(\frac{\partial u}{\partial y} \right) + k \frac{d}{12} \left(\frac{\partial}{\partial t} \frac{\partial^2 u}{\partial y^2} \right) \right]_{ij}^{m}, \qquad (4.9)$$

and we compute an estimate for the frequency μ_y in y-direction, as follows:

$$\mu_y = \frac{\zeta}{h} \sqrt{6 + \frac{6ah\,|\theta_{i,j}^m|}{2d\,|2\gamma_{ij}^m - \gamma_{ij}^{m-1}| + ah\,|\theta_{i,j}^m|}}, \qquad \zeta = \frac{h}{1.05 + 2(d+a)}, \quad (4.10)$$

where

$$\gamma_{ij}^m = u_{ij+1}^m - 2u_{ij}^m + u_{ij-1}^m, \quad \theta_{ij}^m = u_{ij+1}^m - u_{ij-1}^m \qquad (4.11)$$

Although the frequencies of the oscillations in the exact solution are constant, the parameters μ_x and μ_y are estimated at each grid point, so they are particularly adapted to the problem and the selection strategy avoids an extreme accumulation of the global error. It is also worth highlighting that the obtained estimates (4.8) and (4.10) do not affect the computational cost, as it is the case, for instance, of [17, 18, 19, 21], because they do not require numerical solvers for algebraic equations or numerical optimization strategies, but only rely on values already computed.

5 Numerical experiments

In this section we provide the numerical evidence arising from the application of the developed scheme to some test problems based on selected advection-reaction-diffusion equations. In the remainder, we refer to the introduced scheme (2.17) as IMEX-EF and to the classic forward-backward Euler method applied to (2.16) as IMEX-class. Moreover, the error is computed with respect to the exact solution.

Example 5.1. We consider the following problem

$$\frac{\partial u}{\partial t} = \frac{1}{2} \left(\Delta u + \frac{\partial u}{\partial x} + \frac{\partial u}{\partial y} + u - \cos x - \cos y \right), \qquad (5.1)$$

where $u : \left[0, \frac{5\pi}{2}\right]^2 \times [0,1] \longrightarrow \mathbb{R}$, equipped by the initial conditions

$$u(x, y, 0) = \sin x + \sin y, \qquad (5.2)$$

and the boundary conditions

$$\begin{aligned} u(0,y,t) &= \sin y, \quad u\left(\frac{5\pi}{2},y,t\right) = \sin y + 1, \\ u(x,0,t) &= \sin x, \quad u\left(x,\frac{5\pi}{2},t\right) = \sin x + 1. \end{aligned} \tag{5.3}$$

The exact solution is

$$u = \sin x + \sin y,$$

so, it lies in the functional space spanned by trigonometric basis functions (2.2). Therefore, employing the trigonometrically fitted method (2.17) is recommended; the exact values of the parameters μ_x and μ_y in (2.2) are equal to the exact frequencies in the spatial oscillations, i.e. $\mu_x = 1 = \mu_y$.

Figure 1 shows that the numerical solution of problem (5.1) obtained by IMEX-EF method (2.17) oscillates in space with constant shape and speed and is coherent with the boundary conditions. Moreover, IMEX-EF method (2.17) is much more accurate than its classic counterpart IMEX-class, as visible in Table 1. Therefore, also in a very simple case, traditional methods, exact on algebraic polynomials, could require severe stepsize restrictions, strongly increasing the computational cost.

However, the exact values for the parameters are often unknown and their inaccurate estimate could deteriorate the good performances of the IMEX-EF method (2.17), exhibited in Figure 2, where we depict the perturbation added to the exact parameters and the error in the last point. Indeed, the accuracy extremely degrades when the values of the parameters μ_x and μ_y move away from the exact one ($\mu_x = 1 = \mu_y$), reaching almost the accuracy obtained by the classic IMEX for $\mu_x = \mu_{exact} + 10^{-1} = \mu_y$. Moreover, Figure 2 shows that the relation between the introduced perturbation and the error is linear starting from a perturbation equal to 10^{-13}, with almost the equal slope for different choices of spatial mesh width.

Hence, it appears clear how significant is the issue of properly estimating the parameters when their values are not available. In this perspective, we apply the strategy presented in Section 4, which prescribes to approximate the parameters by appropriately manipulating the leading term of the local truncation error. Although the exact spatial frequency is constant, we propose a point-wise computed estimate in order to restrict the accumulation of the global error. As reported in Table 2, IMEX-EF method joined with this estimate is still more accurate than the corresponding classic one.

It is evident that, also for this simple problem, having a solution which oscillates in both spatial directions with the same frequency, the IMEX-EF

method (2.17) achieves higher accuracy with respect to its classic counterpart.

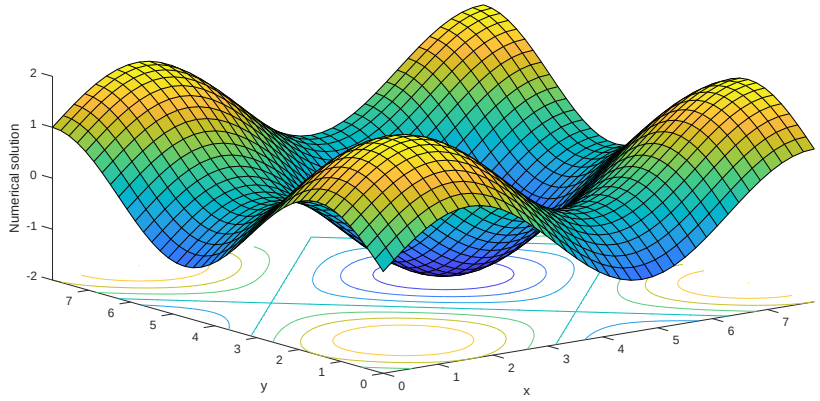

Figure 1: Numerical solution of problem (5.1), with initial conditions (5.2) and boundary conditions (5.3), computed at $t = 1$ by the IMEX-EF method (2.17) with spatial stepsize $h = \pi/16$, time stepsize $k = 0.01$ and the exact value for the parameters, i.e. $\mu_x = 1 = \mu_y$.

Method	**Spatial mesh width**	**Error**
IMEX-EF	$\pi/16$	$7.55 \cdot 10^{-15}$
IMEX-class	$\pi/16$	$5.56 \cdot 10^{-3}$
IMEX-class	$\pi/32$	$1.40 \cdot 10^{-3}$
IMEX-class	$\pi/64$	$3.49 \cdot 10^{-4}$
IMEX-class	$\pi/128$	$8.73 \cdot 10^{-5}$
IMEX-class	$\pi/256$	$2.18 \cdot 10^{-5}$

Table 1: Comparison between the IMEX-EF method (2.17) (combined with the exact values for the parameters, i.e. $\mu_x = 1 = \mu_y$) and its classic counterpart IMEX-class in terms of error computed with respect to the exact solution, within the numerical integration of (5.1) equipped by initial conditions (5.2) and boundary conditions (5.3). The time stepsize is $k = 0.01$.

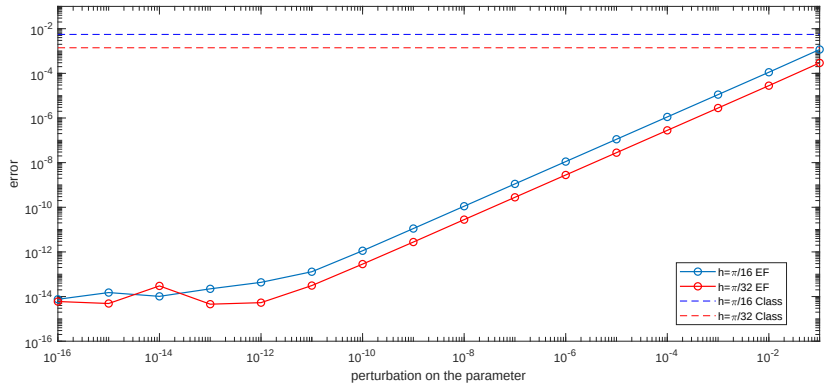

Figure 2: Relation between the perturbation added to the exact parameter ($\mu_x = 1 = \mu_y$) and the error computed in the last point as difference in norm between the exact solution and the numerical solution obtained by the IMEX-EF method within the integration of system (5.1) equipped by initial conditions (5.2) and boundary conditions (5.3), with different spatial mesh width h and time stepsize $k = 0.01$.

Method	$\mu_{\mathbf{x}} = \mu_{\mathbf{y}}$	**Error**
IMEX-EF	1	$7.55 \cdot 10^{-15}$
IMEX-EF	Estimated	$6.69 \cdot 10^{-4}$
IMEX-class	–	$5.56 \cdot 10^{-3}$

Table 2: Accuracy of the IMEX-class method, the IMEX-EF scheme (2.17) applied with the exact value of the parameter ($\mu_x = 1 = \mu_y$) and the IMEX-EF scheme combined with the estimated value (4.8) of the parameter $\mu_x = \mu_y$, for the integration of the problem (5.1) provided with initial conditions (5.2) and boundary conditions (5.3). The spatial grid width is $h = \pi/16$ and the time stepsize is $k = 0.01$.

Example 5.2. Let us consider the following problem having solutions oscillating with different frequencies in the spatial directions:

$$\frac{\partial u}{\partial t} = \frac{1}{4}\left(\Delta u + \frac{\partial u}{\partial x} + \frac{\partial u}{\partial y}\right) + u + \frac{5}{4}\cos 3y - \frac{1}{2}\cos 2x + \frac{3}{4}\sin 3y, \qquad (5.4)$$

where $u : \left[0, \frac{5\pi}{2}\right]^2 \times [0,1] \longrightarrow \mathbb{R}$, equipped by the initial conditions

$$u(x, y, 0) = \sin 2x + \cos 3y, \tag{5.5}$$

and the boundary conditions

$$\begin{aligned} u(0, y, t) &= \cos 3y, \quad u\left(\frac{5\pi}{2}, y, t\right) = \cos 3y + 1, \\ u(x, 0, t) &= \sin 2x + 1, \quad u\left(x, \frac{5\pi}{2}, t\right) = \sin 2x + \frac{\sqrt{2}}{2}. \end{aligned} \tag{5.6}$$

The exact solution is

$$u = \sin 2x + \cos 3y,$$

so, it belongs to the functional space spanned by trigonometric basis functions (2.2). Therefore, it is worthwhile adopting the trigonometrically fitted method (2.17); the exact values for the parameters μ_x and μ_y in (2.2) are equal to the exact frequencies in the spatial oscillations, i.e. $\mu_x = 2$ and $\mu_y = 3$.

As reported in Figure 3, the numerical solution of problem (5.4) obtained by IMEX-EF method (2.17) oscillates in space with constant shape and speed and matches well the boundary conditions. Moreover, the IMEX-EF method (2.17) achieves an higher accuracy than the corresponding IMEX-class, as highlighted in Table 3.

As previously remarked, the exact values for the parameters are often unknown and inaccurately approximating them could extremely reduce the accuracy of the IMEX-EF method (2.17), as shown in Figure 4, where we report the norm of the error in the last point and the perturbation added to exact values of the parameters. Indeed, we observe a lower accuracy when the values of the parameters μ_x and μ_y move away from the exact ones ($\mu_x = 2$ and $\mu_y = 3$), becoming almost the same obtained by IMEX-class for $\mu_x = 2.1$ and $\mu_y = 3.1$, i.e. when the perturbation is equal to 10^{-1}. Moreover, in Figure 4 we observe that the error linearly increases with respect to the perturbation starting from a perturbation equal to 10^{-12}, with a slope that is almost the same with different choices of spatial grid width.

Estimating the parameters through the selection technique described in Section 4, the IMEX-EF scheme is still more accurate than the corresponding classic one, as displayed in Table 4.

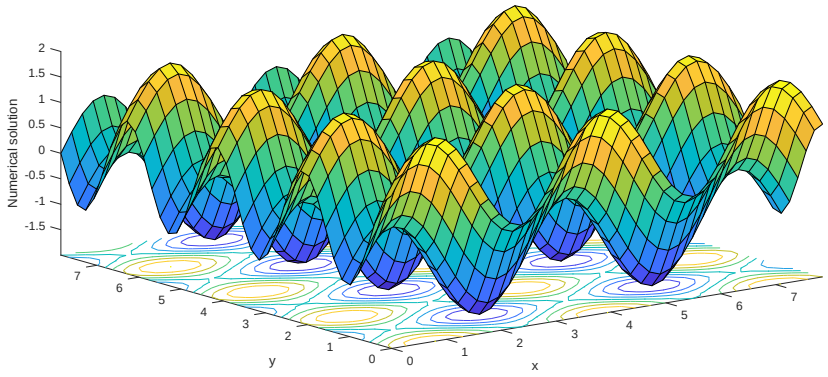

Figure 3: Numerical solution of problem (5.4), with initial conditions (5.5) and boundary conditions (5.6), computed at $t = 1$ by the IMEX-EF method (2.17) with spatial stepsize $h = \pi/16$, time stepsize $k = 0.01$ and the exact values for the parameters, i.e. $\mu_x = 2$ and $\mu_y = 3$.

Method	**Spatial mesh width**	**Error**
IMEX-EF	$\pi/16$	$1.07 \cdot 10^{-14}$
IMEX-class	$\pi/16$	$4.25 \cdot 10^{-2}$
IMEX-class	$\pi/32$	$1.06 \cdot 10^{-2}$
IMEX-class	$\pi/64$	$2.65 \cdot 10^{-3}$
IMEX-class	$\pi/128$	$6.63 \cdot 10^{-4}$
IMEX-class	$\pi/256$	$1.66 \cdot 10^{-4}$

Table 3: Comparison between the IMEX-EF method (2.17) (combined with the exact values for the parameters, i.e. $\mu_x = 2$ and $\mu_y = 3$) and the corresponding IMEX-class, in terms of error with respect to the exact solution, within the numerical integration of (5.4) equipped by initial conditions (5.5) and boundary conditions (5.6). The time stepsize is $k = 0.01$.

6 Conclusions

In this work, we have presented an adapted numerical scheme for advection-reaction-diffusion problems generating periodic wavefronts on a 2D spatial

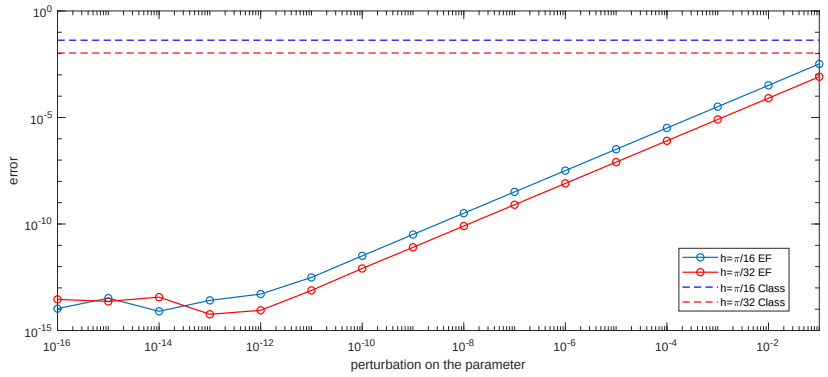

Figure 4: Relation between the perturbation added to the exact parameter ($\mu_x = 2$,$\mu_y = 3$) and the error computed in the last point as difference in norm between the exact solution and the numerical solution obtained by the IMEX-EF method within the integration of system (5.4) provided with initial conditions (5.5) and boundary conditions (5.6), with different spatial mesh width h and time stepsize $k = 0.01$.

Method	$\mu_\mathbf{x}$	$\mu_\mathbf{y}$	**Error**
IMEX-EF	2	3	$2.65 \cdot 10^{-15}$
IMEX-EF	Estimated		$7.61 \cdot 10^{-3}$
IMEX-class	–		$1.04 \cdot 10^{-2}$

Table 4: Accuracy of the IMEX-class method, the IMEX-EF scheme (2.17) applied with the exact values of the parameters ($\mu_x = 2$ and $\mu_y = 3$) and the IMEX-EF scheme combined with the estimated value (4.8) of the parameters μ_x and μ_y, for the integration of problem (5.4) provided with initial conditions (5.5) and boundary conditions (5.6). The spatial mesh width is $h = \pi/32$ and the time stepsize is $k = 0.1$.

domain. It consists in adopting trigonometrically fitted finite differences for the discretization in space, in order to accurately reproduce the prescribed oscillatory behavior of the exact solution along the numerical dynamics. As regards the time integration, it is carried out by the IMEX-Euler method, in order to take the nature of the vector field into account. This problem-oriented approach, introduced in [14], has been extended here to problems defined on a 2D spatial domain and requires facing the crucial problem of

estimating more frequencies in the spatial directions. The estimation here proposed is based on manipulating the local truncation error and do not affect the computational effort required for the overall integration. The effectiveness of the described strategy has also been confirmed via numerical tests. Future issues of this research will regard the adaptation of numerical schemes for deterministic and stochastic evolutionary operators with and without memory [7, 8, 9, 10, 11, 12, 13], such as integral and fractional equations or stochastic oscillators, as well as on problems with spatially quasi-periodic solutions depending on multiple frequencies, also on non-uniform grids.

Acknowledgments
The authors D'Ambrosio and Paternoster are members of the GNCS group. This work is supported by GNCS-INDAM project and by PRIN2017-MIUR project.

References

[1] U. M. Ascher, S. J. Ruuth, B. T. R. Wetton, Implicit-Explicit methods for time-dependent partial differential equations, SIAM J. Numer. Anal., **32,** (1995), 797–823.

[2] R. Araya, E. Behrens, R. Rodriguez, An adaptive stabilized finite element scheme for the advection–reaction–diffusion equation, Appl. Numer. Math., **54,** (2005), 491–503 .

[3] A. R. A. Anderson, M. A. J. Chaplain, E. L. Newman, R. J. C. Steele, A. M. Thompson, Mathematical Modelling of Tumour Invasion and Metastasis, J. Theor. Med., **2,** (2000), 129–151.

[4] U. M. Ascher, S. J. Ruuth, R. J. Spiteri, Implicit-Explicit Runge-Kutta Methods for Time-Dependent Partial Differential Equations, Appl. Numer. Math., **25,** nos.2–3, (1997), 151–167.

[5] S. Boscarino, On an accurate third order implicit-explicit Runge-Kutta method for stiff problems, Appl. Numer. Math., **59,** no. 7, (2009), 1515–1528.

[6] S. Boscarino, Error analysis of IMEX Runge-Kutta methods derived from differential-algebraic systems, SIAM J. Numer. Anal., **45,** no. 4, (2007), 1600–1621.

[7] K. Burrage, A. Cardone, R. D'Ambrosio, B. Paternoster, Numerical solution of time fractional diffusion systems, Appl. Numer. Math., **116,** (2017), 82–94.

[8] A. Cardone, R. D'Ambrosio, B. Paternoster, A spectral method for stochastic fractional differential equations, Appl. Numer. Math., **139,** (2019), 115–119.

[9] C. Chen, D. Cohen, R. D'Ambrosio, A. Lang, Drift-preserving numerical integrators for stochastic Hamiltonian systems, Adv. Comput. Math., **46,** no. 2, (2020), 27.

[10] V. Citro, R. D'Ambrosio, S. Di Giovacchino, A-stability preserving perturbation of Runge-Kutta methods for stochastic differential equations, Appl. Math. Lett., **102,** (2020), 106098.

[11] V. Citro, R. D'Ambrosio, Long-term analysis of stochastic θ-methods for damped stochastic oscillators, Appl. Numer Math., **150,** (2020), 18–26.

[12] D. Conte, R. D'Ambrosio, B. Paternoster, On the stability of ϑ-methods for stochastic Volterra integral equations, Discr. Cont. Dyn. Sys. - Series B, **23,** no. 7, (2018), 2695–2708.

[13] R. D'Ambrosio, M. Moccaldi, B. Paternoster, Numerical preservation of long-term dynamics by stochastic two-step methods, Discr. Cont. Dyn. Sys. - Series B, **23,** no. 7, (2018), 2763–2773.

[14] R. D'Ambrosio, M. Moccaldi, B. Paternoster, Adapted numerical methods for advection-reaction-diffusion problems generating periodic wavefronts, **74,** no. 5, (2017), 1029–1042.

[15] R. D'Ambrosio, B. Paternoster, Numerical solution of reaction-diffusion systems of λ - ω type by trigonometrically fitted methods, J. Comput. Appl. Math., **294(C),** (2016), 436–445.

[16] R. D'Ambrosio, B. Paternoster, Numerical solution of a diffusion problem by exponentially fitted finite difference methods, SpringerPlus, **3,** no. 1, (2014), 425–431.

[17] R. D'Ambrosio, E. Esposito, B. Paternoster, Exponentially fitted two-step Runge-Kutta methods: Construction and parameter selection, Appl. Math. Comp., **218,** no. 14, (2012), 7468–7480.

[18] R. D'Ambrosio, E. Esposito, B. Paternoster, Parameter estimation in exponentially fitted hybrid methods for second order ordinary differential problems, J. Math. Chem., **50,** (2012), 155–168.

[19] R. D'Ambrosio, E. Esposito, B., Paternoster, Exponentially fitted two-step hybrid methods for $y'' = f(x, y)$, J. Comput. Appl. Math., **235,** no. 16, (2011), 4888–4897.

[20] W. Gautschi, Numerical integration of ordinary differential equations based on trigonometric polynomials, Numer. Math., **3,** (1961), 381–397.

[21] D. Hollevoet, M. Van Daele, G. Vanden Berghe, Exponentially-fitted methods applied to fourth order boundary value problems, J. Comput. Appl. Math., **235,** no. 18, (2011), 5380–5393.

[22] W. Hundsdorfer, J. Verwer, Numerical Solution of Time-Dependent Advection-Diffusion-Reaction Equations, Springer-Verlag, 2003.

[23] L. Gr. Ixaru, G. Vanden Berghe, Exponential Fitting, Kluwer, 2004.

[24] E. Isaacson, H. B. Keller, Analysis of Numerical Methods, Dover Publications, 1994.

[25] G. J. McRea, W. R. Goodin, J. H. Seinfeld, Numerical solution of atmospheric diffusion for chemically reacting flows, J. Comput. Phys., **77,** (1982), 1–42.

[26] K. W. Morton, Numerical Solution of Convection-diffusion Problems, Chapman & Hall, 1996.

[27] B. Paternoster, Present state-of-the-art in exponential fitting, A contribution dedicated to Liviu Ixaru on his 70th birthday, Comput. Phys. Commun., **183,** (2012), 2499–2512.

[28] S. J. Ruuth, Implicit-explicit methods for reaction-diffusion problems in pattern formation, J. Math. Biol., **34,** (1995), 148–176.

[29] W. E. Schiesser, The Numerical Method of Lines: Integration of Partial Differential Equations, Academic Press, 1991.

[30] W. E. Schiesser, G. W. Griffiths, A Compendium of Partial Differential Equation Models: Method of Lines Analysis with Matlab, Cambridge University Press, 2009.

[31] G. D. Smith, Numerical solution of partial differential equations - Finite difference methods, Clarendon Press, 1985.

[32] R. Tyson, S. R., Lubkin, J. D. Murray, Model and analysis of chemotactic bacterial patterns in a liquid medium, J. Math. Biol., **38,** (1999), 359–375.

[33] Z. Zlatev, Computer Treatment of Large Air Pollution Models, Kluwer, 1995.

[34] H. Wang, C. W. Shu, Q. Zhang, Stability and Error Estimates of Local Discontinuous Galerkin Methods with Implicit-Explicit Time-Marching for Advection-Diffusion Problems, SIAM J. Numer. Anal., **53,** no. 1, (2015), 206–227.